

Facile Synthesis and Characterization of Aluminum/Graphene Nanosheets Composites

Nashmi H. Alrasheedi¹

Received: 5 May 2015 / Accepted: 6 October 2015 / Published online: 15 April 2016
© King Fahd University of Petroleum & Minerals 2016

Abstract The strength and hardness of the composites were investigated. The present results showed that the strength and hardness of the composites increased with the addition of graphene nanosheets. Graphene nanosheets may act as obstacles for the dislocation movement and finally promote for the dislocations accumulation having an important role for the improvement of mechanical properties of the composites. The difference in thermal expansion coefficient was also responsible for the improvement of the strength and hardness of the composites.

Keywords Metal matrix composites · Graphene nanosheets · Strength · Hardness · Microstructure

1 Introduction

Aluminum Metal Matrix Composites (AMMCs) have received a great interest in the automotive industry compared to steel and iron because of weight reduction which led to both reduced fuel consumption and vehicle emissions [1]. AMMCs were easy to deform and had good electrical and thermal conductivities, high ductility, high strength-to-weight ratio, as well as good corrosion resistance [2]. Hence, they have been widely used in automobile and attract much interest from engineers in the world [3].

Many attempts have been carried out on aluminum–graphite particulate composites [4–6]. It was reported that these

aluminum–graphite composites presented improvement in mechanical properties [7], low friction and wear [8,9], reduced temperature rise at the wearing contact surface [10,11], excellent anti-seizure effects [12,13], improved machinability [14], low thermal expansion and high damping capacity [15,16]. From these characteristics, the aluminum–graphite composites are a potential candidate for automotive and other engineering applications [17]. Lastly, Graphene Nanosheets (GNSs) has been introduced [18]. GNSs consist of several graphene layers, and have similar properties to that of single-layer graphene [19].

Several techniques have been developed for the fabrication of Metal Matrix Composites (MMCs) with high volume fraction of particles such as Powder Metallurgy (PM), Melt Infiltration (MI), electromagnetic separation and spray deposition [20,21]. Among the different processing routes for the production of MMCs, PM through solid-state sintering is particularly suitable for the composites fabrication. PM method presents excellent control over the microstructure, including size, morphology and volume fraction of matrix and reinforcement [22].

Recently, few studies have been carried out on the Al–graphite composites [23–25]. For instance, Rashad et al. [23] reported the effect of low-concentration graphite on mechanical properties of pure aluminum using a semi-powder method. The results showed the improvement of mechanical properties with low-concentration (0.3 wt%) graphite into pure aluminum [23]. Another previous study also reported the effects of sintering temperature and graphite addition on the mechanical properties of aluminum [25]. However, in this study, GNSs were added into aluminum to improve the mechanical properties of the composites. Therefore, the present study is designed to synthesize and characterize the mechanical performance of aluminum reinforced by GNSs.

✉ Nashmi H. Alrasheedi
nashmi.alrasheedi@gmail.com

¹ Department of Mechanical Engineering,
Al Imam Mohammad Ibn Saud Islamic University (IMSIU),
P.O. BOX 5701, Riyadh 11432, Kingdom of Saudi Arabia

2 Experimental Procedures

Aluminum powder with the average particle size of $20\ \mu\text{m}$ and 99.0% purity was used in this experimental work. GNSs with 5–10 nm in thickness and $0.75\text{--}1.5\ \mu\text{m}$ in diameter were used as filler (Fig. 1). The density of aluminum powder and GNSs was 2.7 and $2.0\ \text{g/cm}^3$, respectively.

Aluminum and GNSs were mixed using milling machine at a constant speed of 250 rpm for 15 min. The composite powder was green compacted in a stainless steel mold at room temperature under 400 MPa to obtain the cylindrical composite specimens with the dimension of 0.3 inch both in diameter and height. The specimens were then sintered in the furnace at 500°C for 3 h under air environment. The composites with 0; 2.5 and 5 (all in mass %) GNSs were designated as A, B, and C, respectively.

The structural properties of the sintered composites were identified using an automatic X-ray diffractometer. The experimental density of the composites was measured by the Bouyancy principle. Microstructure of the composites after sintering was observed by Optical Microscopy (OM). The composites were evaluated by compression using universal testing machine with a strain rate of 10^{-4} per second. The composites hardness was measured by applying a load of 200 kgf and holding time of 20 s. A minimum of 3 data points were measured using microhardness.

3 Results

Figure 2 illustrates the X-ray diffraction patterns of the specimens. From Fig. 2, the peak for GNSs is presented at 2θ equal to 26.57° , and confirmed for the presence of GNSs in the composites. The appearance of GNSs peak in this study was consistent with the previous study reported by Leng et al. [26].

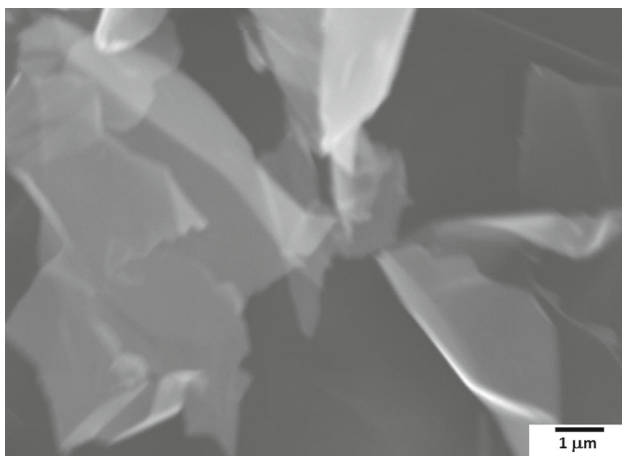


Fig. 1 SEM micrograph of GNSs

Table 1 presents the comparison of theoretical and measured densities of the specimens. Generally, it was clear that the density of the specimens decreased by increasing the GNSs content. Figure 3 demonstrates the relative density of the specimens as a function of GNSs content. It indicated that the addition of GNSs to aluminum decreased the relative density of the specimens, confirming the presence of GNSs promoted the porosity formation.

Figure 4 shows the optical micrographs of the specimens after sintering at 500°C for 3 h. The specimen A reveals a slight coarse structure where the grain size was large enough (Fig. 4a). The specimen B showed a finer structure compared to the specimen A and had relatively homogenous structure (Fig. 4b). For specimen C, its microstructure was quite similar to the specimen B, but the agglomerates was still found as indicated by arrows (Fig. 4c). The average grain size was approximately $47\ \mu\text{m}$ for specimen A, $35\ \mu\text{m}$ for specimen B and $24\ \mu\text{m}$ for specimen C. From this point of view, it can be realized that the addition of GNSs into aluminum may promote finer structure after sintering (Fig. 4b, c).

Figure 5 shows the compression strength of the specimens as a function of GNSs content. The addition of 2.5 mass% GNSs to aluminum (specimen B) resulted in the increase of the compression strength for about 25% compared to the specimen A. Meanwhile, the addition of 5 mass% GNSs to aluminum (specimen C) was still increased the strength of the composites, but its increment is not as significant as the specimen B. Furthermore, the hardness of the specimens demonstrated a similar trend to its strength as shown in Fig. 6.

4 Discussion

From Table 1, it is obvious that the theoretical density has higher value compared to the measured density. The theoret-

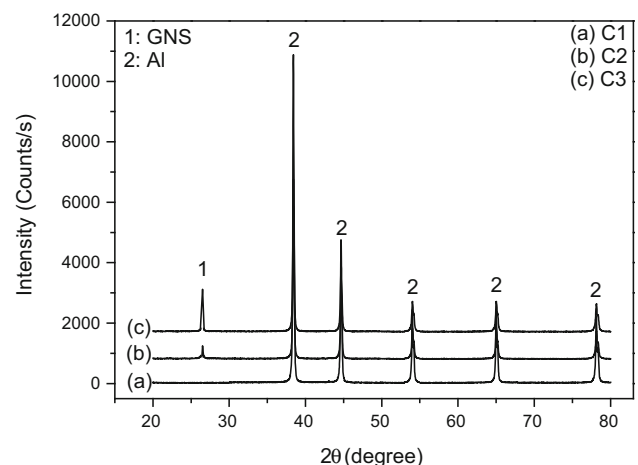


Fig. 2 X-ray diffraction patterns of the specimens

Table 1 Theoretical and experimental densities of the specimens

Specimens	Theoretical density (g/cm ³)	Measured density (g/cm ³)	
		Compacted	Sintered
A	2.70	2.696	2.673
B	2.646	2.631	2.542
C	2.553	2.548	2.409

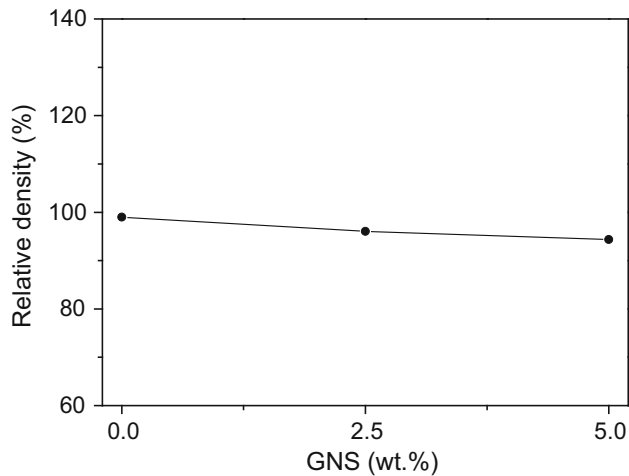


Fig. 3 Relative density of the specimens

ical density (ρ_{theo}) of the composite can be measured using the method reported by Zhai et al. [27]. Note that High sintering temperature facilitates the diffusion of atoms leading to better sinterability of the composites [28].

The optical micrographs demonstrated the reduction in grain size of the specimens (Fig. 4). It is considered that the addition of GNSs into aluminum exerted a retarding force or pressure on the grain boundaries, known as Zener drag, which may retard the grain growth of the structures [29]. Therefore, the ability to suppress the grain growth can be assessed by considering a random spatial relationship between the boundaries and the particles [30].

The distribution of GNSs in aluminum can cause an inhibition of the plastic flow of the matrix and this causes the increased strength and hardness of the composites [31]. The addition of GNSs into aluminum also decreased the distance among the particles, which may act as obstacles for the dislocation movement, leading to the dislocation accumulation. It is known as dispersion-strengthening [32]. Accordingly, it can be thus understood that the increase in the GNSs content results in reducing the distance between GNSs particles which improved the strength and hardness of the specimens [33].

Furthermore, it is also considered that the difference in thermal expansion coefficient between GNSs (10^{-6} K^{-1}) and aluminum ($23.6 \times 10^{-6} \text{ K}^{-1}$) is quite large. The increase

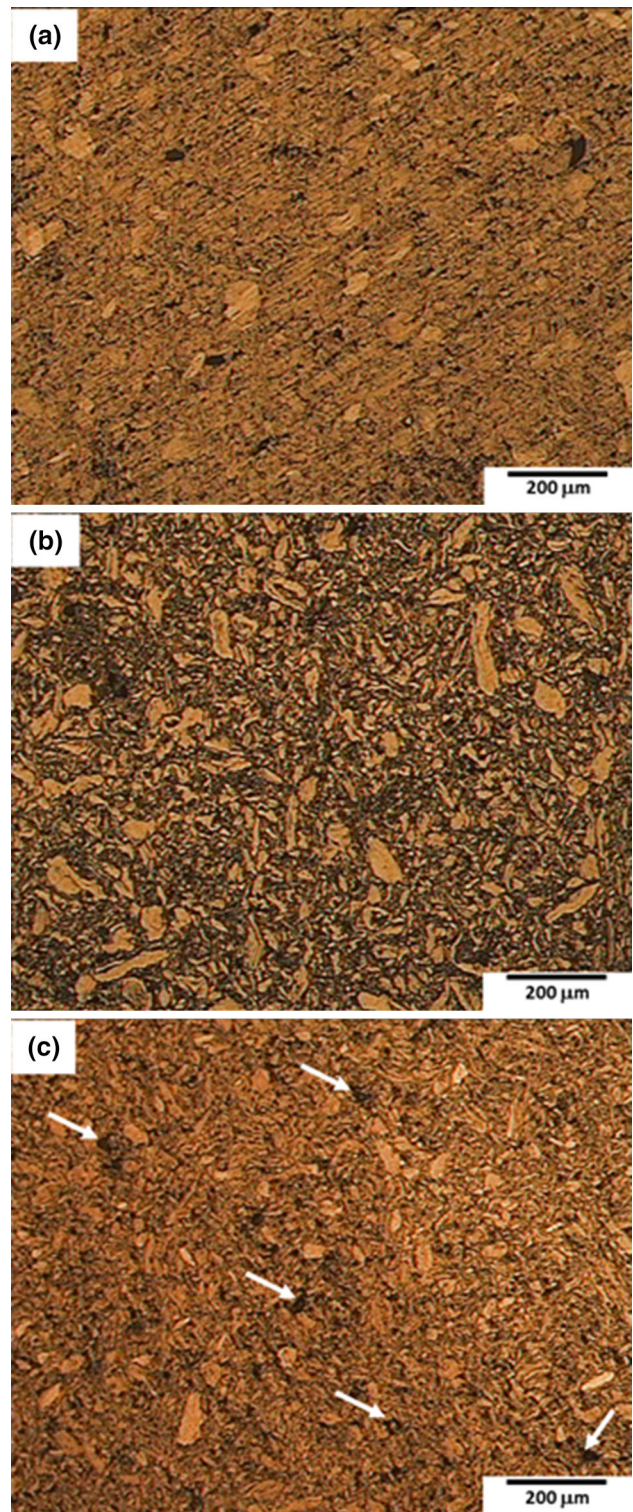


Fig. 4 Optical micrographs of the specimens after sintering at 500 °C for 3 h

in the yield strength of the composites owing to the difference in thermal expansion coefficient ($\Delta\sigma_{CTE}$) can be expressed as follow [34]:

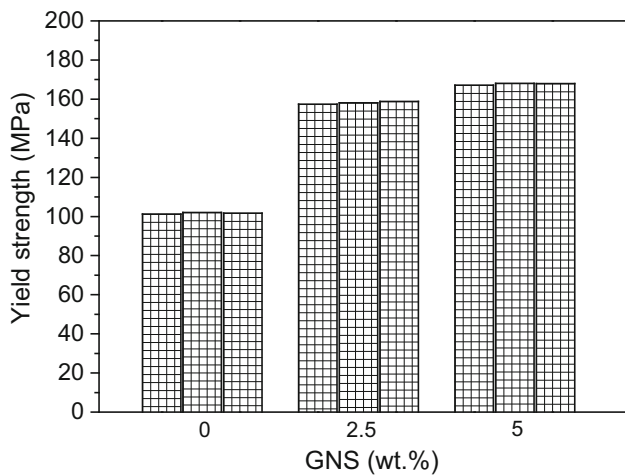


Fig. 5 Yield strength of the specimens

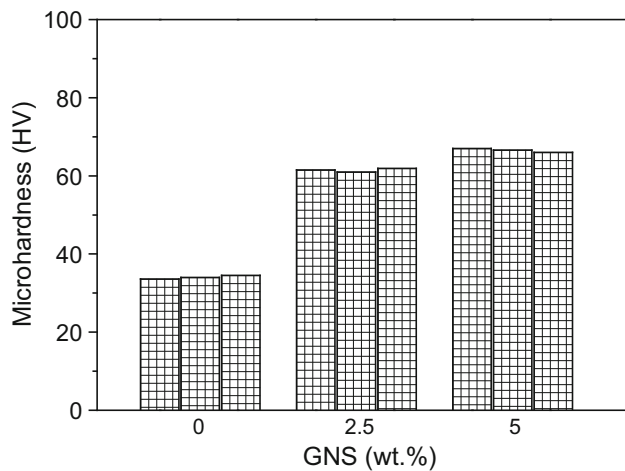


Fig. 6 Microhardness of the specimens

$$\Delta\sigma_{CTE} = \alpha Gb(12 \Delta T \Delta C f_v / b d_p)^{1/2} \quad (1)$$

where $\Delta\sigma_{CTE}$ is the change in yield strength due to thermal expansion coefficient; α is a constant (its value is 1.25); G is the shear modulus of Al matrix; b is burger vector of the matrix; ΔT is temperature change; ΔC is difference of thermal expansion coefficient between matrix and GNSs; f_v is volume fraction of the GNSs particles; and d_p is mean particle size of GNSs.

5 Conclusions

The addition of GNSs has delivered the force or pressure which suppresses the grain growth, leading to the finer structure due to the addition of GNSs. Generally, the addition of GNSs had greatly improved the strength and hardness of the composites. The incorporation of GNSs into aluminum diminished the distance among the particles, where they may

act as obstacles for the dislocation movement and obtain the dislocation accumulation. The increase of strength and hardness of the composites was also attributed to the significant difference in thermal expansion coefficient between GNSs and aluminum.

Acknowledgement The author would like to extend his sincere appreciation to the Department of Mechanical Engineering, University of Arkansas at Fayetteville, USA for the facilities.

References

1. Prasad, S.V.; Asthana, R.: Aluminum metal-matrix composites for automotive applications: tribological considerations. *Tribol. Lett.* **17**, 445 (2004)
2. Oso'rio, W.R.; Cheung, N.; Peixoto, L.C.; Garcia, A.: Corrosion resistance and mechanical properties of an Al 9wt% Si alloy treated by laser surface remelting. *Int. J. Electrochem. Sci.* **4**, 820 (2009)
3. Bahrami, A.; Razaghian, A.; Emamy, M.; Khorshidi, R.: The effect of Zr on the microstructure and tensile properties of hot-extruded Al–Mg₂Si composite. *Mater. Des.* **36**, 323 (2012)
4. Pedersen, L.M.; Bentzen, J.J.; Bramsø, N.: Dimensional response of metal matrix graphite particle composites to sintering. *Scr. Mater.* **44**, 743 (2001)
5. Akhlaghi, F.; Pelaseyyed, S.A.: Characterization of aluminum/graphite particulate composites synthesized using a novel method termed "In situ powder metallurgy". *Mater. Sci. Eng. A* **385**, 258 (2004)
6. Flores-Zamora, M.I.; Estrada-Guel, I.; Gonzalez-Hernandez, J.; Miki-Yoshida, M.; Martinez-Sanchez, R.: Aluminum–graphite composite produced by mechanical milling and hot extrusion. *J. Alloys Compd.* **434**(435), 518 (2007)
7. Ge, D.; Gu, M.: Mechanical properties of hybrid reinforced aluminum based composites. *Mater. Lett.* **49**, 334 (2001)
8. Ted Guo, M.L.; Tsao, C.Y.A.: Tribological behavior of self-lubricating aluminum/SiC/graphite hybrid composites synthesized by the semi-solid powder densification method. *Compos. Sci. Technol.* **60**, 65 (2000)
9. Ted Guo, M.L.; Tsao, C.Y.A.: Tribological behavior of aluminum/SiC/nickel-coated graphite hybrid composites. *Mater. Sci. Eng. A* **333**, 134 (2002)
10. Rohatgi, P.K.; Asthana, R.; Das, S.: Solidification structures and properties of cast metal–ceramic particle composites. *Int. Met. Rev.* **31**, 115 (1986)
11. Ames, W.; Alpas, A.T.: Wear mechanisms in hybrid composites of graphite-20% SiC in A356 aluminum alloy. *Metall. Mater. Trans. A* **26**, 85 (1995)
12. Chu, H.S.; Liu, K.S.; Yeh, J.W.: An in situ composite of Al (graphite, Al₄C₃) produced by reciprocating extrusion. *Mater. Sci. Eng. A* **277**, 25 (2000)
13. Rohatgi, P.K.; Pai, B.C.: Seizure resistance of cast aluminium alloys containing dispersed graphite particles of various sizes. *Wear* **59**, 323 (1980)
14. Rohatgi, P.: Cast aluminum–matrix composites for automotive applications. *J. Mech.* **43**, 10 (1991)
15. Wei, J.N.; Cheng, H.F.; Zhang, Y.F.; Han, F.S.; Zhou, Z.C.; Shui, J.P.: Effects of macroscopic graphite particulates on the damping behavior of commercially pure aluminum. *Mater. Sci. Eng. A* **325**, 444 (2002)
16. Rohatgi, P.K.; Nath, D.; Singh, S.S.; Keshavaram, B.N.: Factors affecting the damping capacity of cast aluminium-matrix composites. *J. Mater. Sci.* **29**, 5975 (1994)

17. Rohatgi, P.K.; Ray, S.; Liu, Y.: Tribological properties of metal matrix graphite particle composites. *Int. Mater. Rev.* **37**, 129 (1992)
18. Park, S.; Ruoff, R.: Chemical methods for the production of graphenes. *Nat. Nanotechnol.* **4**, 217 (2009)
19. Liu, X.; Wei, D.; Zhuang, L.; Cai, C.; Zhao, Y.: Fabrication of high-strength graphene nanosheets/Cu composites by accumulative roll bonding. *Mater. Sci. Eng. A* **642**, 1 (2015)
20. Xiao, B.I.; Bi, J.; Zhao, M.J.; Ma, Z.Y.: Effects of SiCp size on tensile property of aluminum matrix composites fabricated by powder metallurgical method. *Acta Metall. Sinica* **38**, 1006 (2002)
21. Huang, Y.D.; Froyen, L.; Wevers, M.: Quality control and non-destructive tests in metal matrix composites. *J. Nondestruct. Eval.* **20**, 113 (2001)
22. Harrigan, W.C. Jr.: Commercial processing of metal matrix composites. *Mater. Sci. Eng. A* **244**, 75 (1998)
23. Rashad, M.; Pan, F.; Tang, A.; Asif, M.: Effect of graphene nanoplatelets addition on mechanical properties of pure aluminum using a semi-powder method. *Prog. Nat. Sci.* **24**, 101 (2014)
24. Wang, J.; Li, Z.; Fan, G.; Pan, H.; Chen, Z.; Zhang, D.: Reinforcement with graphene nanosheets in aluminum matrix composites. *Scr. Mater.* **66**, 594 (2012)
25. Bustamante, R.P.; Morales, D.B.; Martinez, J.B.; Guel, I.E.; Sanchez, R.M.: Microstructural and hardness behavior of graphene-nanoplatelets/aluminum composites synthesized by mechanical alloying. *J. Alloys Compd.* **615**, S578–S582 (2012)
26. Leng, J.; Wu, G.; Zhou, Q.; Dou, Z.; Huang, X.L.: Mechanical properties of SiC/Gr/Al composites fabricated by squeeze casting technology. *Scr. Mater.* **59**, 619 (2008)
27. Zhai, W.C.; Zhang, Z.H.; Wang, F.C.; Shen, X.B.; Lee, S.K.; Wang, L.: Effect of Si content on microstructure and properties of Si/Al composites. *Trans. Nonferrous Met. Soc. China* **24**, 982 (2014)
28. Yeoh, A.; Persad, C.; Eliezer, Z.: Dimensional responses of copper-graphite powder composites to sintering. *Scr. Mater.* **37**, 271 (1997)
29. Loodgard, L.; Ryum, N.: Precipitation of dispersoids containing Mn and or Cr in Al–Mg–Si alloys. *Mater. Sci. Eng. A* **283**, 144 (2000)
30. Nes, E.; Ryum, N.; Hunderi, O.: On the Zener drag. *Acta Metall.* **33**, 11 (1985)
31. Razaghian, A.; Yu, D.; Chandra, T.: Fracture behaviour of a SiC-particle-reinforced aluminium alloy at high temperature. *Compos. Sci. Technol.* **58**, 293 (1996)
32. Lagerpusch, U.; Mohles, V.; Nembach, E.: On the additivity of solid solution and dispersion strengthening. *Mater. Sci. Eng. A* **319**(321), 176 (2001)
33. Torralba, J.M.; da Costa, C.E.; Velasco, F.: P/M aluminum matrix composites: an overview. *J. Mater. Proc. Technol.* **133**, 203 (2003)
34. Miller, W.S.; Humphreys, F.J.: Strengthening mechanisms in particulate metal matrix composites. *Scr. Metall. Mater.* **25**, 33 (1991)

